

VALIDATION OF A MULTI-SEGMENT FOOT AND ANKLE KINEMATIC MODEL FOR PEDIATRIC GAIT

K.A. Myers¹, M. Wang¹, R.M. Marks², G.F. Harris^{1,2}

¹Department of Biomedical Engineering, Marquette University, Milwaukee, WI, USA

²Department of Orthopaedic Surgery, Medical College of Wisconsin, Milwaukee, WI, USA

Abstract- This paper quantifies the system characteristics for a pediatric foot and ankle biomechanical model. While orientated along the Z-axis the static system resolution is computed at 0.32 ± 0.29 mm with 99.9% accuracy. Dynamic resolution and accuracy are 0.43 ± 0.39 mm and 99.8%, respectively. Angular dynamic resolution computes to 0.52 ± 3.36 degrees at 99.6% accuracy. These calculations are comparable to the Milwaukee adult foot and ankle model.

Keywords – Foot, ankle, kinematics, pediatric, biomechanics

I. INTRODUCTION

The foot and ankle is a complex structural system. Motions at joints during gait are a function of bony repositioning. The foot serves to support and propel the body, transfer forces from the ground, and provide rotation for adaptations on uneven terrain. Dysfunctions of the foot have numerous origins broadly categorized as either injury or pathology. It is crucial to properly treat foot and ankle dysfunction, as it may lead to pain, further dysfunction, and erosion of proximal ability.

A currently accepted approach to quantifying foot and ankle kinematics is to represent the entire foot as a single rigid body with a revolute ankle joint. While useful for overall sagittal plane studies, this method is inadequate for portraying true 3-D motion. More sophisticated models that segment the foot further and provide multi-planar rotation offer valuable insight into the segmental foot kinematics.

Few models include multi-segmental kinematics during both the stance and swing periods of gait. More typically, the biomechanical foot model is constrained to a limited number of segments and includes rotational limitations that restrict joint motion to a single axis of rotation [2], [5], [6], [7]. Such rotational limitations are unable to track well documented, multi-axis joint rotations [3]-[5], [7], [8].

With regard to the pediatric population, there are very few biomechanical models that assess foot and ankle motion. As with the adult populations of interest, pediatric models of the foot and ankle strive to accurately describe the complex kinematics of foot motion in order to better understand kinematic pathology and to improve treatment. Challenges in developing appropriate pediatric foot models include small foot sizes and close marker spacing, which frequently exceeds the capabilities of the motion analysis system.

The objective of this study was to develop an accurate biomechanical foot and ankle model to describe the kinematics of pediatric gait during both stance and swing. It was hypothesized that the pediatric system could function with equivalent or greater resolution, accuracy, and reliability when compared to existing adult foot and ankle model systems.

II. METHODOLOGY

A. Foot and Ankle Model

The biomechanical model defines the foot and ankle as four distinct segments: 1) tibia and fibula, 2) talus and calcaneus, 3) distal tarsals and metatarsals, and 4) hallux (Fig. 1). Each rigid body segment is coupled by an unrestricted 3-D joint to the next distal segment.

B. Instrumentation

A 15 camera VICON 524 (Oxford Metrics, Oxford, England) motion analysis system was used to acquire 3-D marker data at 120 Hz. The capture volume was defined with dimensions of 1.3 m (height) by 1.0 m (width) by 4.9 m (length). This volume ensured collection of complete stance and swing phase gait data. Three markers were placed on bony landmarks (Fig. 2) to define each segment of the model. The markers are small ($d = 14.5$ mm), lightweight, and covered with reflective tape.

For the dynamic testing procedures, a Biodex System 3 (Biodex Medical Systems, Inc., New York, USA) was used to generate defined angular rotations.

C. Validation Protocol

Resolution and accuracy of the foot and ankle system was determined both statically and dynamically [1], [3], [26]. For static linear testing, four markers were placed on a dummy segment representing the approximate shortest and longest inter-marker distances of the pediatric foot and ankle model. A mid-point distance was also explored. The marker positions were measured with a vernier caliper (± 0.02 mm tolerance). The dummy segment was placed in the capture volume and oriented

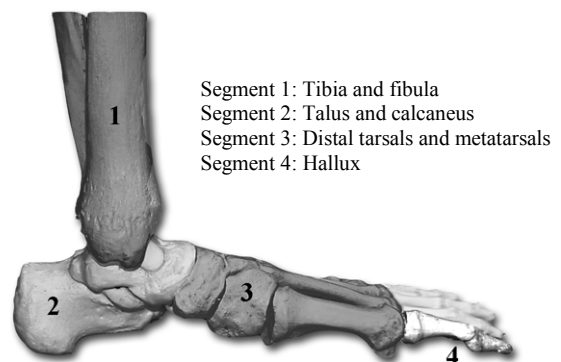


Fig. 1. Bones of the foot and ankle with their associated model segment

Report Documentation Page

Report Date 25OCT2001	Report Type N/A	Dates Covered (from... to) -
Title and Subtitle Validation of a Multi-Segment Foot and Ankle Kinematic Model for Pediatric Gait	Contract Number	
	Grant Number	
	Program Element Number	
Author(s)	Project Number	
	Task Number	
	Work Unit Number	
Performing Organization Name(s) and Address(es) Department of Biomedical Engineering, Marquette University, Milwaukee, WI	Performing Organization Report Number	
Sponsoring/Monitoring Agency Name(s) and Address(es) US Army Research, Development & Standardization Group (UK) PSC 802 Box 15 FPO AE 09499-1500	Sponsor/Monitor's Acronym(s)	
	Sponsor/Monitor's Report Number(s)	
Distribution/Availability Statement Approved for public release, distribution unlimited		
Supplementary Notes Papers from the 23rd Annual International Conference of the IEEE Engineering in Medicine and Biology Society, October 25-28, 2001, held in Istanbul, Turkey. See also ADM001351 for entire conference on cd-rom.		
Abstract		
Subject Terms		
Report Classification unclassified	Classification of this page unclassified	
Classification of Abstract unclassified	Limitation of Abstract UU	
Number of Pages 3		



Fig.2. Marker locations.

$$t_{\text{origin}} = \begin{bmatrix} (M2_x + M3_x)/2 \\ (M2_y + M3_y)/2 \\ (M2_z + M3_z)/2 \end{bmatrix}$$

$$t'_2 = \begin{bmatrix} M3_x - t_{\text{origin},x} \\ M3_y - t_{\text{origin},y} \\ M3_z - t_{\text{origin},z} \end{bmatrix}$$

$$t'_1 = t' \times \begin{bmatrix} M1_x - t_{\text{origin},x} \\ M1_y - t_{\text{origin},y} \\ M1_z - t_{\text{origin},z} \end{bmatrix}$$

$$t'_3 = t'_1 \times t'_2 \quad T = [t'_1 \ t'_2 \ t'_3]$$

along either the x, y, or z global reference system axis. Data was collected for 6 trials of 3 sec duration for each orientation. The testing procedures were then repeated two days later.

Dynamic linear testing was done by taking the same dummy segment and moving it through the capture volume at an average gait speed. Finally, dynamic angular testing was done by using the Biodex System 3 (accuracy = 0.67%) to rotate through a known range. The system provided the required angular output over time and was compared to the biomechanical model output at various positions in the range.

System resolution was calculated from the following equation [3]:

$$R = /D - \frac{1}{n} \sum_{i=0}^{n-1} d_i / \pm t \left(\frac{s}{\sqrt{n}} + \varepsilon_r + \varepsilon_m \right)$$

With D = measured distance

n = total number of samples

d_i = computed distance

t = t-test coefficient (from statistical tables [10])

s = sample standard deviation

ε_r = round-off error = $(5/10^m)$

ε_m = measurement error, based on micrometer resolution (± 0.02 mm).

m = number of significant digits.

System accuracy was computed as [3]:

$$A = \left(1 - \frac{1/x_w - \frac{1}{n} \sum_{i=0}^{n-1} d_i}{\frac{1}{n} \sum_{i=0}^{n-1} d_i} \right) \times 100\%$$

With A = percentage system accuracy

x_w = "worst" data point.

The biomechanical model used a series of Euler rotations to determine the angle of the dummy segment rotating with respect to the Biodex. The order of rotation was chosen to be in the sagittal, coronal, and then transverse planes of motion. Each segment was assigned its own axis system. For instance, the dummy left tibia segment is defined as:

T is the 3x3 rotation matrix for the left tibia segment comprised of the three unit vectors, t'_1 , t'_2 and t'_3 . One segment can be expressed relative to the adjacent segment by multiplying the transpose 3x3 rotation matrix of the proximal segment by that of the distal segment.

III. RESULTS

The results of the static linear testing are shown in Table I. Markers placed at 140.7 mm represent the long distance, 70.5 mm represent the mid distance, and 39.9 mm represent the shortest distance. For comparative statistical purposes, t-test coefficients were selected at the 0.05 and 0.01 levels of significance. Table II summarizes the results of the dynamic linear testing. The markers were oriented along the Z-axis for the trials. Table III shows the computations of resolution and accuracy for the dynamic angular testing. The Biodex was programmed to rotate at a rate of 180 deg/sec. The positions of rotation were measured at a constant angular velocity of 180 deg/sec.

ORIENTATION	MARKER POSITION	ACCURACY	RESOLUTION (MM)	P-VALUE
X-axis	Short	100 %	.30 ± .141	.05
			.30 ± .236	.01
	Mid	100 %	.50 ± .141	.05
			.50 ± .236	.01
	Long	99.98 %	.417 ± .175	.05
			.417 ± .291	.01
Y-axis	Short	100 %	.60 ± .141	.05
			.60 ± .236	.01
	Mid	99.90 %	.533 ± .184	.05
			.533 ± .306	.01
	Long	100 %	.10 ± .141	.05
			.10 ± .236	.01
Z-axis	Short	99.95 %	.183 ± .175	.05
			.183 ± .291	.01
	Mid	99.88 %	.317 ± .174	.05
			.317 ± .292	.01
	Long	99.94 %	.483 ± .175	.05
			.483 ± .292	.01

Table I. Static Linear Resolution and Accuracy Testing Results

MARKER POSITION	ACCURACY	RESOLUTION (MM)	P-VALUE
Short	99.84 %	0.533 ± .189	.05
		0.533 ± .315	.01
Mid	99.81 %	0.433 ± .236	.05
		0.433 ± .394	.01
Long	99.91 %	0.233 ± .236	.05
		0.233 ± .394	.01

Table II. Dynamic Linear Resolution and Accuracy Testing Results

POSITION	X-AXIS		Y-AXIS		Z-AXIS	
	Resolution (mm)	Accuracy	Resolution (mm)	Accuracy	Resolution (mm)	Accuracy
1	.828 ± 3.56	99.39%	.412 ± 3.50	99.19 %	.22 ± 3.57	99.18 %
2	.288 ± 3.42	99.66 %	.248 ± 3.58	99.56 %	.091 ± 3.90	98.92 %
3	1.03 ± 3.35	99.77 %	.556 ± 3.54	99.64 %	.518 ± 3.36	99.75 %
4	1.17 ± 3.81	99.81 %	.932 ± 3.43	99.81 %	.108 ± 3.35	99.87 %
5	.99 ± 3.50	99.82 %	2.32 ± 3.62	99.67 %	2.96 ± 3.53	99.83 %

Table III. Dynamic Angular Test Results with Biodex velocity = 180°/sec and p=. 01 level of significance.

IV. DISCUSSION

For the results of the linear static testing, the resolution was slightly greater when the segment was oriented along the Z-axis. Accuracy values are acceptable regardless of orientation or testing procedure. The comparable adult foot and ankle system reported static resolution as 0.01 ± 1.20 mm with an accuracy of 99.4% (assuming a 0.01 level of significance) in the sagittal plane [3]. The coronal resolution for the adult model was 0.6 ± 1.10 mm with 99.5% accuracy. Transverse plane information was not provided. For the dynamic testing, resolution increased with decreasing marker distance. This result is typical of most imaging systems. However, the resolution for the short marker separation is still in a satisfactory range. Results from Kidder et al. document average resolution along the X-axis as 0.65 ± 0.07 mm and average accuracy as 98.9% [3]. Y and Z-axis resolution and accuracy are 0.95 ± 0.08 at 98.8% and 0.98 ± 0.13 at 99.0%, respectively, at a 0.05 level of significance [3].

V. CONCLUSION

The static and dynamic test results confirm the system accuracy and ability to track 3-D motion during pediatric gait. The resolution and accuracy computations are comparable, and even surpass similar measurements for an existing adult foot and ankle model. The dynamic angular test results also verify the ability of the biomechanical model to track rotations accurately. (Few models publish this measurement, so a comparison is not obtainable.) In light of the current study results, the model is considered sufficient for further application in a pilot clinical

study of pediatric foot and ankle motion. It is hoped that quantification of normal and pathological pediatric gait will ultimately lead to improved characterization, rehabilitation, and surgical treatment.

REFERENCES

- [1] M.P. Kadaba, M.E. Wooten, H.K. Ramakrishnan, D. Hurwitz, and G.V. B. Cochran, "Assessment of human motion with VICON," *ASME Biomechan Symp.*, vol. 84, pp. 335-338, 1989.
- [2] T.M. Kepple, S. J. Stanhope, K.N. Lohmann, and N.L. Roman, "A video based technique for measuring ankle-subtalar motion during stance," *J Biomech Eng.*, vol. 105, pp. 136-144, 1983.
- [3] S.M. Kidder, F.S. Abuzzahab, G.F.Harris, and J.E. Johnson, "A system for the analysis of foot and ankle kinematics during gait," *IEEE Trans Rehab Eng.*, vol. 4, pp. 25-32, 1996.
- [4] A. Leardini, M.G. Benedetti, F. Catani, L.Simoncini, and S. Giannini, "An anatomically based protocol for the description of foot segments during gait," *Clin Biomech.*, vol. 14, pp. 528-536, 1999.
- [5] S. H. Scott and D. A. Winter, "Talocalcaneal and talocalcaneal joint kinematics and kinetics during the stance phase of walking," *J Biomech.*, vol.24, pp. 743-752, 1991.
- [6] S. H. Scott and D. A. Winter, "Biomechanical model of the human foot: kinematics and kinetics during the stance phase of walking," *J Biomech.*, vol.26, pp. 1091-1104, 1993.
- [7] K.L. Seigal, T.M. Kepple, P.G. O'Connell, L.H. Gerber, and S.J. Stanhope, "A technique to evaluate foot function during the stance phase of gait," *Foot & Ankle*, vol. 16, pp. 764-770, 1995.
- [8] T. Stahelin, B.M. Nigg, D.J. Stafanyshyn, A.J. van den Bogart, and S.J. Kim, "A method to determine bone movement in the ankle joint complex *in vitro*," *J Biomech.*, vol. 30, pp. 513-516, 1997.
- [9] M.W. Whittle, "Calibration and performance of a 3-dimensional television system for kinematic analysis," *J Biomech.*, vol. 15, pp. 185-196, 1982.
- [10] L. Ott, *An Introduction to Statistical Methods and Data Analysis*. Boston, MA: PWS-Kent, 1988, p.A5.